The Astrophysical Journal Letters, 918:L11 (5pp), 2021 September 1 https://doi.org/10.3847/2041-8213/ac1db4

Brightness Temperature Constraints on Coherent Processes in Magnetospheres of Neutron Stars

Maxim Lyutikov
Department of Physics and Astronomy, Purdue University, 525 Northwestern Avenue, West Lafayette, IN 47907-2036, USA; lyutikov@purdue.edu
Received 2021 July 9; revised 2021 August 7; accepted 2021 August 16; published 2021 August 26

Abstract

We discuss constraints that the observed brightness temperatures impose on coherent processes in pulsars and fast radio bursts, and in particular on the hypothesis of coherent curvature emission by bunches. We estimate the peak brightness temperature that a bunch of charge Ze can produce via synchrotron and/or curvature emission as $k_{\rm B}T \sim (Ze)^2/\lambda$, where λ is the typical emitted wavelength. We demonstrate that the bunch's electrostatic energy required to produce observed brightness temperature is prohibitively high, of the order of the total *bulk* energy. We compare corresponding requirements for the free-electron laser mechanism and find that in that case the constraints are more easily satisfied.

Unified Astronomy Thesaurus concepts: Pulsars (1306); Radio transient sources (2008); Radio bursts (1339)

1. Introduction

Many modern-day theories of coherent emission from pulsars/fast radio burst (FRBs) accept the "coherent curvature emission by bunches" model, formulated in the early years of pulsar research (Goldreich & Keeley 1971; Cheng & Ruderman 1977), and go on calculating the details of this assumption. Extensive work in the 1970s through today (Benford & Buschauer 1977; Asseo et al. 1990; Melrose 1992; Melrose & Gedalin 1999; Melrose et al. 2021) demonstrated that the model is not viable.

The problems are many. For example, in the original version of Goldreich & Keeley (1971), the bunching, driven by a weak radiation-reaction effect, is easily destroyed by minor velocity spread. Another problem is the long times needed to create the bunches: in a relativistically streaming plasma the processes in the beam frame are suppressed both by smaller rest-frame beam/plasma density if compared with the lab frame, and relativistic freezing of any corresponding dynamical process as viewed in the lab frame (e.g., Lyutikov 1999).

Here we approach the question "How justified is the assumption of the coherent emission by bunches?" from the observational side: let us assume that bunches are created. What is the corresponding conditions to reproduce the observed properties? In particular, creation of electrostatically repulsive bunches costs energy. How much? Are the costs consistent with the model? (The answer is no.)

As a quantitative parameter that would measure the validity of the model we take the (awkwardly defined but universally used) quantity of brightness temperature. (Energetics is typically not an issue since radio carries minuscule amount of energy, though observations of FRBs start to impose meaningful constraints on the plasma parameters at the source; Lyutikov & Rafat 2019.)

In case of pulsars and FRBs the brightness temperatures reach values in excess of 10^{35} K (e.g., Manchester & Taylor 1977; Melrose 2000; Lorimer et al. 2007), and as high as $\sim 10^{40}$ K in extreme cases (e.g., Soglasnov et al. 2004). Can models of coherent emission by bunches reproduce those brightness temperatures?

We limit our approach to the class of an "antenna" mechanism (as opposed to a plasma maser; Lyutikov et al. 1999; Melrose & Gedalin 1999). That is, all particles emit independently, but due to the external driver they all emit in phase. We also limit our consideration to models operating within the magnetospheres of neutron stars: simultaneous observations of radio and X-ray bursts (Bochenek et al. 2020; CHIME/FRB Collaboration et al. 2020; Mereghetti et al. 2020; Ridnaia et al. 2021) unequivocally establishes magnetospheric origin of FRBs, as argued by Lyutikov & Popov (2020).

Cyclotron and curvature emission are qualitatively very similar, but there is an important observational distinction: small cyclotron times typically cannot be resolved by the observing instruments; hence, we see emission averaged over many gyration periods. Emitted and observed powers are equal then (if no bulk motion). Curvature emission is different: a particle emits once when its velocity is nearly along the line of sight. At that moment it is moving relativistically toward an observer, so emitted and observed powers are different.

We illustrate the above points with three examples: a more familiar synchrotron emission (Section 2.1) and a popular model of coherent curvature emission by bunches (Section 2.2), and the recently proposed free-electron laser (FEL) mechanism (Section 3).

2. Peak Brightness Temperatures of Synchrotron and Curvature Emission

2.1. Single Particle

Let's start with the more familiar case of synchrotron emission. This involves a subtle difference between the emitted power and the observed one (e.g., Scheuer 1968). The *average* synchrotron power *emitted* by a particle (we stress the "averaged" and the "emitted"—not "instantaneously observed") is

$$P_{a,s} \approx \frac{e^2}{c}\gamma^2\omega_{\rm B}^2 \tag{1}$$

and typical frequency

$$\omega_s \sim \gamma^2\omega_{\rm B}$$
$$\omega_{\rm B} = \frac{eB}{m_e c}. \tag{2}$$

(For the sake of clarity we omit factors of unity.)

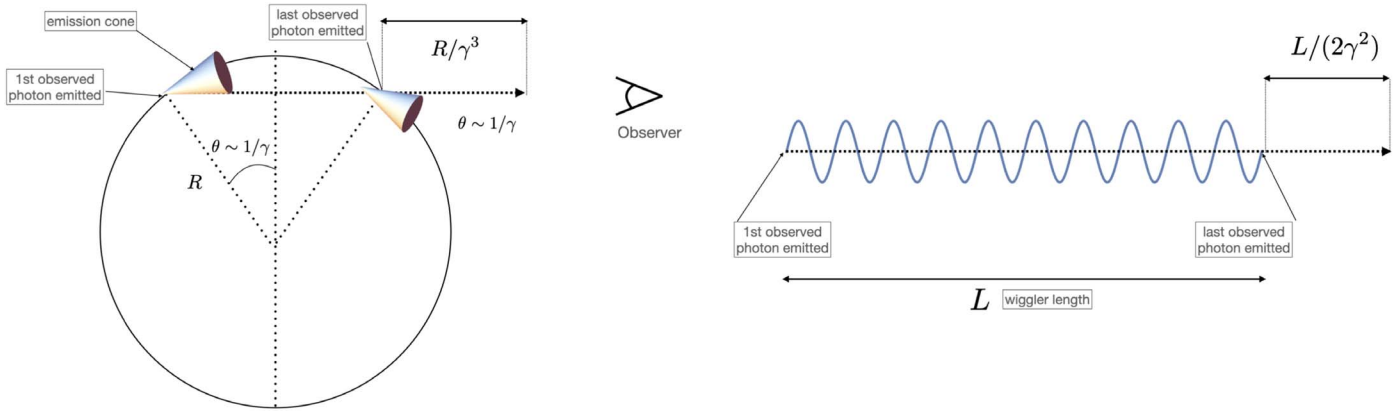

Figure 1. Illustration of the difference between emitted and observed powers for synchrotron/curvature emission when viewed on an orbital timescale (left panel) and FEL emission (right panel). In the case of synchrotron/curvature emission the particle is moving clockwise along the circle with radius R and Lorentz factor γ. It emits toward an observer for a time $\sim 2(R/c)/\gamma$, but the first and last observed photons arrive within $\sim 2(R/c)/\gamma^3$. For $\gamma \gg 1$ the curvature of the trajectory is a higher-order effect. In the case of an FEL wiggler of length L and particles propagating "to the right" all the emitted photons are concentrated with a region of $\sim L/(2\gamma^2)$. For an electromagnetic wiggler propagating "to the left" the interaction time and burst duration are further reduced by $1+\beta \approx 2$.

It can be derived from the relativistic Larmor formula for intensity of radiation

$$P_a = \frac{2}{3} e^2 \gamma^6 \left(a_\parallel^2 + \frac{1}{\gamma^2} a_\perp^2 \right), \tag{3}$$

where $a_\parallel$ and $a_\perp$ are acceleration along and perpendicular to the velocity. The quantity P_a is the rate of energy loss by an electron seen in the lab frame at the moment when the electron has given velocity and acceleration, as measured in the lab frame.

For a particle on Larmor orbit with

$$r_L = \gamma \frac{c}{\omega_B} \tag{4}$$

the period of rotation and transverse acceleration are

$$T_{rot} = \gamma \frac{2\pi}{\omega_B}$$
$$a_\perp = \frac{c^2}{r_L} = \frac{c\omega_B}{\gamma}. \tag{5}$$

Hence we derive relation (1).

Relation (3) is the power *emitted* by an electron. It equals the *average* power seen by an observer stationary with respect to the gyration center, modulo angular factors of the order of unity —not dependent on the particle Lorentz factor (in a sense that an observer measuring energy flux through a given surface area, and projecting the result over the whole sky, would infer emitted power $\sim P_a$). In other words, it is an integrated power seen by all observers spread out over 4π.

For an observer in the gyration plane that average power comes in the form of bursts, when the direction of electron motion nearly coincides with the line of sight, see Figure 1.

A relativistic particle emits within a cone of $\sim 1/\gamma$. Hence, a particle emits toward an observer for a period

$$t_{em} \sim \frac{1}{\gamma} T_{rot} \sim \frac{1}{\omega_B}. \tag{6}$$

Note that the radiation formation length

$$l_r \sim \gamma^2 \lambda \sim c/\omega_B \ll r_L \tag{7}$$

is comparable to ct_{em}.

As the particle within a small angle $\sim 1/\gamma$ nearly catches up with its radiation, the observed pulse duration

$$t_{ob} \sim \frac{t_{em}}{\gamma^2} = \frac{2\pi}{\gamma^2 \omega_B}. \tag{8}$$

Note that the inverse/Fourier transform of (8) gives the typical frequency (2).

Now, energy emitted during time (6) is

$$E_{em} = \frac{e^2}{c} \gamma^2 \omega_B. \tag{9}$$

And the observed power

$$P_{ob} = \frac{E_{em}}{t_{ob}} \sim \frac{e^2}{c} \gamma^4 \omega_B^2. \tag{10}$$

This is power during the peak emission in the middle of a short pulse. The peak power is γ^2 times larger than the average (1). This is the difference between emitted and observed power. Qualitatively, an observer sees one short bright burst per period of rotation. The peak brightness is much larger than the average one, by $\sim \gamma^2$. In other words, all the energy we observe is emitted during $1/\gamma$ fraction of the orbit, but it arrives within a time span $1/\gamma^2$ shorter.

Peak observed spectral power

$$P_{ob,\omega} = \frac{P_{ob}}{\omega_s} \sim \frac{e^2}{c} \gamma^2 \omega_B. \tag{11}$$

Estimating the brightness temperature as

$$k_B T_b \sim P_{ob,\omega} \frac{c}{(\omega t_{ob})^2} \tag{12}$$

we find

$$k_B T_b \approx \frac{e^2}{\lambda}$$
$$\lambda = \frac{c}{\omega}. \tag{13}$$

Relation (13) give the effective brightness temperature during a burst of synchrotron emission for a single electron producing synchrotron emission at wavelength λ. Thus, the brightness temperature of the emission peak of synchrotron and of the curvature emission is approximately the electrostatic energy with the emitted wavelength.

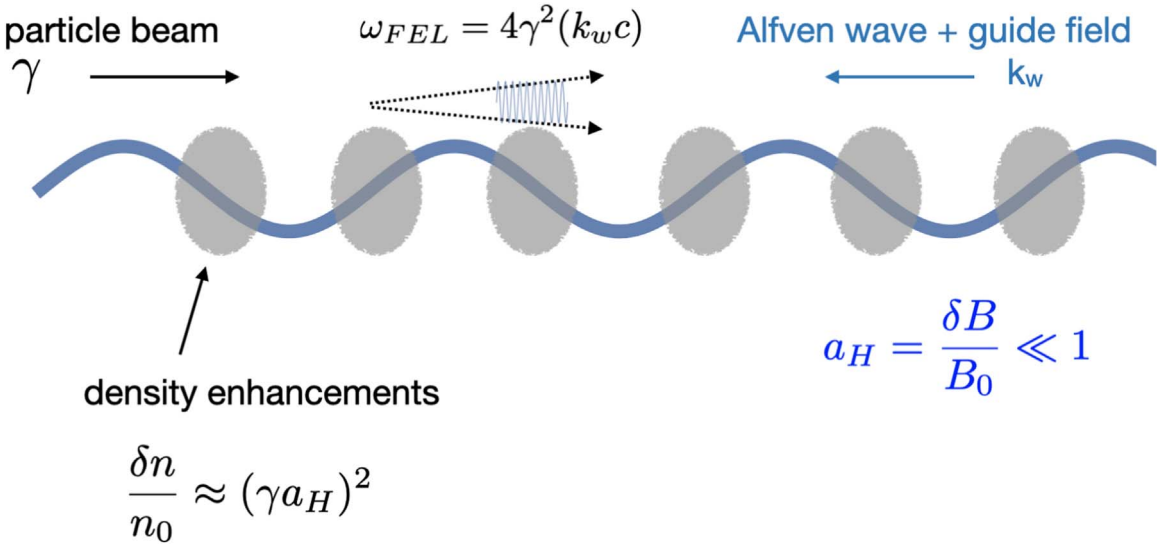

Figure 2. Cartoon of the FEL model of production of coherent emission. An Alfvén wave (a wiggler) with wavenumber k_w is propagating to the left with relative amplitude a_H (Equation (21)). A beam of particles propagates to the right. In the guide-field-dominated regime particles move mostly along the magnetic field with velocity fluctuating at the double frequency; this creates density enhancements that coherently Compton/Raman scatter the Alfvén wave.

A numerical estimate gives

$$T_b = 5 \times 10^{-5} \nu_9 \text{ K}, \tag{14}$$

where $\nu_9 = \nu/10^9$ is the frequency of the emitted waves in GHz.

The procedure outlined above to estimate the peak brightness temperature for synchrotron emission gives *the same* brightness temperature for the curvature emission as well (Equation (13)). Note that the observed peak power of curvature emission,

$$P_{\text{ob},c} \sim \frac{e^2}{c} \gamma^6 \left(\frac{c}{R_c}\right)^2, \tag{15}$$

is different from the emitted power by a factor γ^2.

2.2. Coherent Curvature Emission by Bunches

The antenna mechanism is qualitatively based on the idea that if there is a bunch of Z electrons that has a dimension smaller than a wavelength $\leqslant \lambda$, it will produce an emission pulse with brightness temperature

$$k_{\text{B}} T_b \approx Z^2 \frac{e^2}{\lambda}. \tag{16}$$

Scaling with $\propto Z^2$ indicates coherent process. Hence, the number of electrons needed in a bunch to produce a given brightness temperature T_b is

$$Z = \frac{\sqrt{k_{\text{B}} T_b \lambda}}{e} = 2.5 \times 10^{16} T_{b,30}^{1/2} \lambda^{1/2}, \tag{17}$$

where we normalized brightness temperature to 10^{30} K, an appropriate scaling for pulsars and FRBs.

Importantly, relation (16) gives an estimate of the electrostatic Coulomb energy $E_{\text{Cmb,curv}}$ required to create one bunch[1]:

$$E_{\text{Cmb,curv}} \sim k_{\text{B}} T_b \sim 10^{14} T_{b,30} \text{ erg}. \tag{18}$$

[1] The corresponding equipartition magnetic field, assuming that the bunch occupies volume $\sim \lambda^3$, is

$$B \sim \frac{\sqrt{k_{\text{B}} T_b}}{\lambda^{3/2}} = 5 \times 10^7 \frac{T_{b,30}^{1/2}}{\lambda^{3/2}} \text{ G}.$$

The ratio of electrostatic energy to create a bunch to the bulk kinetic energy of the bunch $E_k \sim \gamma Z m_e c^2$,

$$\frac{E_{\text{Cmb,curv}}}{E_k} \approx \left(\frac{1}{\gamma} \frac{(k_{\text{B}} T_b)}{m_e c^2} \frac{r_e}{\lambda}\right)^{1/2} = \left(\gamma \frac{(k_{\text{B}} T_b)}{m_e c^2} \frac{r_e}{R_c}\right)^{1/2}. \tag{19}$$

Assuming that $R_c \sim c/\Omega$, numerical estimates give

$$\frac{E_{\text{Cmb,curv}}}{E_k} = 7 \nu_9^{1/6} T_{b,30}^{1/2}. \tag{20}$$

The Crab pulsar with period 0.03 s is near the light cylinder. For broader applications, the ratio $(r_e/R_c)^{1/2}$, Equation (19), microscopic to macroscopic parameters, does not vary much by changing the macroscopic one.

Relation (20) is the main result: the electrostatic energy required to created charge bunches to produce coherent curvature emission of observed brightness temperature is prohibitively high, of the order of the total *bulk* energy.

Finally, we note that the model of "coherent emission by bunches" cannot be taken to the continuous limit (this would eliminate the extra γ^2 factor in the observed power). A constant flow of particles, even a charged one, will not produce any radiation.

3. FEL mechanism

Lyutikov (2021) developed a model of FEL for the production of coherent emission in pulsars (Crab in particular) and FRBs (Figure 2). The model has many attractive features, including an explanation for some very subtle observed relationships: (i) it operates in a very broad range of the neutron star's parameters (*independent* of the value of the magnetic field); (ii) it can tolerate mild momentum spread of the beam $\Delta p/p \leqslant 1$; (iii) it reproduces (multiple) emission bands seen in Crab and FRBs, and can also produce broader emission; (iv) it gives correct estimates for the brightness temperatures both in pulsars and FRBs; (v) it explains the correlation between polarization and spectral properties (that narrowband emission in FRBs are correlated with linear polarization).

The model assumes that Alfvén waves (electromagnetic wigglers) with relative amplitude

$$a_H = \frac{\delta B}{B_0} \ll 1. \tag{21}$$

(δB is the fluctuating magnetic field and B_0 is the guiding field) and wavenumber k_w propagates through the neutron star magnetosphere. The wiggler shakes the electron beam. The resulting ponderomotive force, appearing due to the beat of the wiggler and the electromagnetic wave amplified via parametric resonance, leads to the creation of charged bunches. The powerful wiggler then shakes the bunches producing coherent emission.

Single particle emitted power and frequency are

$$\begin{aligned} P_{a,\mathrm{FEL}} &\approx a_H^2 \frac{e^2}{c}\gamma^4 (k_w c)^2 \\ \omega_{\mathrm{FEL}} &\sim \gamma^2 (k_w c). \end{aligned} \tag{22}$$

Thus, the wiggler is Compton scattered by the beam (FEL in the guide-field-dominated regime cannot be treated as curvature emission in a wiggled field).

The emitting particle continuously propagates toward an observer—this is an important difference from the synchrotron and curvature emission (when the observer sees a short burst).

Consider emission from a particle propagating in a static wiggler of length L (relations are the same, within a factor of $\sim$2, for the electromagnetic wiggler propagating toward the particle), so that a particle emits for time L/c; but in the observer frame this is shorter by γ^2. Total emitted energy is $\sim P_{a,\mathrm{FEL}} L/c$ and $t_{\mathrm{ob}} \sim L/(\gamma^2 c)$. The observed power is thus

$$P_{\mathrm{ob,FEL}} \approx a_H^2 \frac{e^2}{c}\gamma^6 (k_w c)^2. \tag{23}$$

The peak spectral power

$$P_\omega = \frac{P_{\mathrm{ob,FEL}}}{\omega_{\mathrm{FEL}}} = a_H^2 e^2 \gamma^4 k_w = a_H^2 \frac{e^2}{c}\gamma^2 \omega. \tag{24}$$

The brightness temperature of the observed pulse is then

$$k_{\mathrm{B}} T_b = a_H^2 \gamma^8 \frac{e^2 c^2 k_w}{L^2 \omega^2} = \left(\frac{\gamma a_H}{\eta_w}\right)^2 \frac{e^2}{\lambda}. \tag{25}$$

where we normalized the total wiggler length to the fluctuating wavenumber, $L = \eta_w / k_w$, $\eta_w \gg 1$. (Factor $\gamma a_H/\eta_w$ is typically $\leqslant 1$.)

The required bunching number Z to produce given brightness temperature is

$$Z \approx \frac{\eta_w}{\gamma a_H} \frac{\sqrt{k_{\mathrm{B}} T_b \lambda}}{e}. \tag{26}$$

The charged bunches in the FEL need not be static ones—this involved huge energy as we discussed above. The charged bunches can be dynamic (e.g., Langmuir oscillations driven by the wiggler for FEL operating in the Raman regime), so here there is no need to confine them electrostatically. Still, let us take an extreme view and following the previous estimates demonstrate that FEL is consistent even with the extreme case of statically produced charged bunches.

The corresponding electrostatic energy

$$E_{\mathrm{Cmb},w} \sim Z^2 \frac{e^2}{\lambda} = \left(\frac{\eta_w}{\gamma a_H}\right)^2 k_{\mathrm{B}} T_b \tag{27}$$

(we used $\lambda k_w \sim 1/\gamma^2$). In absolute values the quantity $E_{\mathrm{Cmb},w}$ is larger than $E_{\mathrm{Cmb,curv}}$, (18) since the factor in front of $k_{\mathrm{B}} T_b$ is generally larger than unity.

Ratio of electrostatic energy over kinetic energy

$$\begin{aligned} \frac{E_{\mathrm{Cmb},w}}{E_k} &= \frac{\eta_w}{a_H} \frac{\sqrt{k_{\mathrm{B}} T_b} k_w \sqrt{\lambda}}{m_e c^2} \\ &= \left(\frac{\eta_w}{a_H}\right) T_{30}^{1/2} \sqrt{\lambda} \times \begin{cases} 2 \times 10^{-4} & \text{Crab light cylinder} \\ 3 \times 10^{-2} & \text{near neutron star.} \end{cases} \end{aligned} \tag{28}$$

(wavelength λ is not normalized—as measured in centimeters). A smaller ratio of electrostatic to beam energy in this case can be traced to the fact that the frequency of curvature emission scales as γ^3, while FEL scales as γ^2—hence, for a similar scale of $\sim$light cylinder, in the case of curvature emission γ is smaller, and therefore smaller bulk energy.

Most importantly, in the case of the FEL the bunching is driven, in some correctly implied sense, not by the beam but by the wiggler (the axial bunching force $\propto \delta v \delta B$, while the velocity drift component δv is also $\propto \delta B$).

The ratio of electrostatic to wiggler energy within λ^3, $E_w \sim a_H^2 B_0^2 c \lambda^3$, evaluates to

$$\begin{aligned} \frac{E_{\mathrm{Cmb},w}}{E_w} &= \frac{\eta_w^2}{a_H^4} \frac{k_{\mathrm{B}} T_b k_w}{B_0^2 \lambda^2} = \left(\frac{\eta_w^2}{a_H^4}\right) T_{30} \lambda^{-2} \\ &\times \begin{cases} 10^{-6} & \text{at Crab lightcylinder} \\ 10^{-19} b_q^{-2} & \text{near magnetar} \end{cases}, \end{aligned} \tag{29}$$

where $b_q = B_0/B_Q$ and $B_Q = m_e^2 c^3/(\hbar c)$. Scaling to the quantum magnetic field B_Q is given since the model of Lyutikov (2021) applies both to the inner regions of magnetars and the Crab's light cylinder. Thus, mild wigglers can indeed create (have enough energy for) the required charged bunches.

4. Discussion

In this Letter we argue that a popular simple model of "coherent curvature emission by bunches" is not self-consistent: the price in electrostatic energy that is needed to create charge bunches is too high to explain the observed brightness temperatures. This is our main conclusion.

Together with the well-recognized problems of how to create charge bunches (Benford & Buschauer 1977; Asseo et al. 1990; Melrose 1992; Melrose & Gedalin 1999; Melrose et al. 2021), the unrealistic energetic requirements further assert that coherent emission by bunches is not a viable pulsar/FRM emission mechanism.

On a more general issue, we point out an apparently subtle confusion in the literature between the emitted power and the observed one. The former can be measured in the electron rest frame; the latter depends on the location of the observer. Though synchrotron and curvature emission are qualitatively very similar, the cyclotron motion is typically very fast, so that the use of the average power (1) is basically justified. If there is no bulk motion of plasma, then the *average* observed power equals *average* emitted power. This is not the case for curvature emission:

particles stream along the field lines and appear in the line of sight once. At this moment the observed power is different from the emitted power by a factor $\sim \gamma^2$. This is an important correction to the *observed* power of curvature radiation.

This work had been supported by NASA grants 80NSSC17K0757 and 80NSSC20K0910 and NSF grants 1903332 and 1908590. I would like to thank Mikhail Medvedev and Alexandre Philippov for discussions.

ORCID iDs

Maxim Lyutikov https://orcid.org/0000-0001-6436-8304

References

Asseo, E., Pelletier, G., & Sol, H. 1990, MNRAS, 247, 529
Benford, G., & Buschauer, R. 1977, MNRAS, 179, 189
Bochenek, C. D., Ravi, V., Belov, K. V., et al. 2020, Natur, 587, 59
Cheng, A. F., & Ruderman, M. A. 1977, ApJ, 212, 800
CHIME/FRB Collaboration, Andersen, B. C., Bandura, K. M., et al. 2020, Natur, 587, 54
Goldreich, P., & Keeley, D. A. 1971, ApJ, 170, 463
Lorimer, D. R., Bailes, M., McLaughlin, M. A., Narkevic, D. J., & Crawford, F. 2007, Sci, 318, 777
Lyutikov, M. 1999, JPlPh, 62, 65
Lyutikov, M. 2021, arXiv:2102.07010
Lyutikov, M., Machabeli, G., & Blandford, R. 1999, ApJ, 512, 804
Lyutikov, M., & Popov, S. 2020, arXiv:2005.05093
Lyutikov, M., & Rafat, M. 2019, arXiv:1901.03260
Manchester, R. N., & Taylor, J. H. 1977, Pulsars (San Francisco, CA: W. H. Freeman)
Melrose, D. B. 1992, RSPTA, 341, 105
Melrose, D. B. 2000, in ASP Conf. Ser. 202, IAU Coll. 177: Pulsar Astronomy —2000 and Beyond, ed. M. Kramer, N. Wex, & R. Wielebinski (San Francisco, CA: ASP), 721
Melrose, D. B., & Gedalin, M. E. 1999, ApJ, 521, 351
Melrose, D. B., Rafat, M. Z., & Mastrano, A. 2021, MNRAS, 500, 4530
Mereghetti, S., Savchenko, V., Ferrigno, C., et al. 2020, ApJL, 898, L29
Ridnaia, A., Svinkin, D., Frederiks, D., et al. 2021, NatAs, 5, 372
Scheuer, P. A. G. 1968, ApJL, 151, L139
Soglasnov, V. A., Popov, M. V., Bartel, N., et al. 2004, ApJ, 616, 439